

Cloning of PC3B, a Novel Member of the PC3/BTG/TOB Family of Growth Inhibitory Genes, Highly Expressed in the Olfactory Epithelium

Pasquale Buanne,* Giuseppina Corrente,* Laura Micheli,* Antonella Palena,†
 Patrizia Lavia,† Corrado Spadafora,‡ Madepalli Krishnappa Lakshmana,*
 Alessandra Rinaldi,§ Sandro Banfi,[¶] Michæla Quarto,[¶]
 Alessandro Bulfone,[¶] and Felice Tirone*^{¶1}

*Istituto di Neurobiologia and §Istituto di Tecnologie Biomediche, CNR, Viale Marx 43, 00137 Rome, Italy; †Centro di Genetica Evoluzionistica, Via degli Apuli, 00100 Rome, Italy; ‡Istituto Superiore di Sanità, Viale Regina Elena 299, Rome, Italy; and [¶]Telethon Institute of Genetics and Medicine (TIGEM), Via Olgettina 58, 20132 Milan, Italy

Received April 10, 2000; accepted June 12, 2000

We identified in the EST database murine and human sequences similar, but not identical, to the members of the PC3/BTG/TOB family of cell cycle inhibitors. A conserved domain (aa 50–68) of the PC3 protein, the prototype member of the family, was used as a query. That domain has been shown by us to be necessary for the antiproliferative activity of PC3. A murine EST clone and a highly homologous human EST clone, containing the entire ORF, were chosen for sequencing. Comparison to databases and a phylogenetic tree analysis indicated that these EST clones are the mouse and human homologues of a gene that represents a novel member of the PC3/BTG/TOB family. This gene, named PC3B, is endowed with marked antiproliferative activity, being able to induce G₁ arrest, and is highly expressed in testis, in oocyte, and in preimplantation embryos. Analysis of its expression during murine development indicated a specific localization in the olfactory epithelium at midgestation, suggesting that PC3B might be involved in the differentiation of this neuronal structure. Human PC3B mapped to chromosome 11q23, as indicated by radiation hybrid analysis. © 2000 Academic Press

INTRODUCTION

The PC3B gene described in this report is a novel member of a family of negative regulators of the cell cycle. The founding member of this family is represented by the gene PC3, originally isolated by us as an immediate-early gene activated at the onset of neuronal differentiation in rat PC12 cells by nerve growth

factor (NGF; Bradbury *et al.*, 1991). The murine homologue, named TIS21, was identified as a tetradecanoyl phorbol acetate-induced transcript in mouse NIH3T3 cells by the Herschman group (Fletcher *et al.*, 1991). PC3 is expressed in proliferating neuroblasts within the germinal zone of the neural tube, at the moment of the last proliferative cycle preceding differentiation into a mature neuron (Iacopetti *et al.*, 1994, 1999). This finding led us to hypothesize that PC3 might exert a negative control on proliferation, acting *in vivo* when the neuroblast becomes committed to differentiation (Iacopetti *et al.*, 1994). Such a hypothesis was also consistent with a report that described a novel sequence named BTG1, with 60% identity to PC3, endowed with antiproliferative properties (Rouault *et al.*, 1992). We ascertained that PC3 was able to inhibit proliferation in neuronal PC12 cells and in NIH3T3 cells by inducing G₁ arrest through the conversion of pRb—a key growth inhibitory molecule of the cell cycle—into its active form (Montagnoli *et al.*, 1996; Guardavaccaro *et al.*, 2000). The antiproliferative properties of the human homologue of PC3, named BTG2, have also been analyzed (Rouault *et al.*, 1996). Furthermore, it was shown that BTG2 was induced by the key regulatory cell cycle gene, p53, and that ES cells in which PC3/TIS21/BTG2 had been genetically ablated underwent apoptosis and failed to arrest in G₂ phase upon induction of DNA damage. This suggested that PC3/TIS21/BTG2 had a role in cell survival after genotoxic damage (Rouault *et al.*, 1996).

After the cloning of PC3/TIS21/BTG2 and of BTG1, novel related antiproliferative genes were isolated, namely TOB (Matsuda *et al.*, 1996), murine BTG3 (Guehenneux *et al.*, 1997) and its human homologue ANA (Yoshida *et al.*, 1998), and human TOB2 (Ikematsu *et al.*, 1999). These genes share about 60, 40, 35, and 33% sequence identity with PC3, respectively. A

Sequence data from this article have been deposited with the EMBL/GenBank Data Libraries under Accession Nos. AJ005120 (murine Pc3b) and AJ271351 (human PC3B).

¹ To whom correspondence should be addressed. Telephone: 39-6-86895963. Fax: 39-6-86090370. E-mail: tirone@mercury.itbm.rm.cnr.it.

common feature among all these genes is their ability to inhibit proliferation. More recently, other related genes, as judged by sequence similarity, were identified, and their sequences were made available in the GenBank database.

All the protein sequences of the family are quite similar, with two regions of higher conservation, corresponding to aa 50–68 and 96–115 in PC3. However, TOB and TOB2 extend at the carboxy-terminal region further than the other proteins of the family, their homology being limited to the amino-terminal domain. The carboxyl-terminal domain of TOB interacts with the mitogenic receptor p185^{erbB2}, which is able to counteract the antiproliferative effect of TOB (Matsuda *et al.*, 1996). This suggests that, within a common functional role of the whole gene family in cell cycle control, specific molecular targets could be defined by additional domains of the protein, as might be the case for TOB. However, no homology to known functional motifs is evident in the cDNA-deduced proteins of these genes, thus leaving open the question about their specific molecular function. Recent findings concerning PC3/BTG2/TIS21 indicated that this gene (and hence, possibly the other genes of the family) acts as a transcriptional regulator, as it is able to arrest G₁ to S phase progression by inhibiting cyclin D1 transcription (Guardavaccaro *et al.*, 2000). Furthermore, BTG2 was shown to interact with the mCAF1 gene, i.e., the mouse homologue of the yeast CAF/POP2 gene (Rouault *et al.*, 1998), which is part of the yeast CCR4 protein, a component of a multisubunit complex required for the regulation of several genes (Liu *et al.*, 1997).

The novel PC3B gene, whose cloning and characterization are presented here, has clear antiproliferative properties and a specific pattern of expression in development, suggesting that it might play specific functional roles within the PC3/BTG/TOB family.

MATERIALS AND METHODS

Sequence analysis and computer-assisted search of databases. Automated fluorescence DNA sequencing was performed using Perkin-Elmer 377 Prism machines with Dye Terminator Sequencing chemistries on double-strand plasmid templates. Computer analyses of the sequences were performed with the Wisconsin Package version 10.0-UNIX of the Genetics Computer Group (GCG), Madison, Wisconsin (January 1999). Similarity searches were performed using BlastN, BlastP, and FastA algorithms, against the GenBank (release 113, August 1999), EMBL (release 59.0, June 1999), Pir-Protein (release 61.0, June 1999), and Swiss-Prot (release 38.0, July 1999) databases.

Construction of PC3B vectors. An expression vector for murine Pc3b was generated by subcloning into the *EcoRV* site of the vector pcDNA3 (Clontech) the fragment *MluI* (5')–*SalI* (3') from the mouse cDNA clone 944385, blunted after excision. The mouse pcDNA-Pc3b vector was used for the proliferation assays. The same construct, after

excision of the AT-rich 150-bp fragment *HindIII*–*HindIII* at the 3' end, was used to generate ³⁵S-labeled CTP probes for *in situ* hybridization.

Northern analysis. Two micrograms of mRNA from mouse and human tissues, blotted on a nylon filter, was hybridized as previously described (Buanne *et al.*, 1998) with mouse or human PC3B cDNA probes that were ³²P-labeled following the hexamer primer method (Feinberg and Vogelstein, 1983). The mRNA amounts were controlled by hybridizing the filters to a β -actin probe.

Mice. Mating of C57/B16 mice and the definition of embryo stages were as described (Buanne *et al.*, 1998). The protocol by Zaccagnini *et al.* (1998) was followed for collection of oocytes from superovulated B6D2F1 females, *in vitro* fertilization, and embryo culture to the blastocyst stage.

RNA extraction and RT-PCR assays. RNA was extracted from oocytes, morulae, and blastocysts using TRIZOL reagent (Gibco BRL). RT-PCRs were carried out using the SuperScript One-Step RT-PCR System (Gibco BRL), according to the manufacturer's instructions. Parallel reactions were performed replacing the RT/*Taq* with *TaqI* polymerase (Gibco BRL), to exclude the presence of contaminating genomic DNA. Murine Pc3b-specific primers had the following sequences: forward, 5'-ACGGCGGTCCTCTGAAGCCT-3'; reverse, 5'-ATGACTGGCCTCCCTGC-3'. The reaction efficiencies and the initial amount of RNA template in each reaction were assessed using commercial primers specific for β -actin (Stratagene). The following PCR conditions were used: 1 cycle at 50°C for 30 min followed by 2 min at 94°C; 40 cycles of denaturation (1 min at 94°C), annealing (1 min at 60°C), and elongation (1 min at 68°C); a final extension step for 7 min at 68°C. One-fourth of each PCR was electrophoresed through 2% agarose gels, blotted on nylon filters, and hybridized using [γ -³²P]ATP-labeled internal oligonucleotides (sequences: 5'-AGGAGATGACCATATGGG-3' for Pc3b and 5'-AGAGAGGTATCCTGACCCTGAAGTAC-3' for β -actin). PCR products were visualized by autoradiography (see also Montagnoli *et al.*, 1996).

In situ hybridization. Expression was detected in tissue sections of embryonic day 10.5 (E10.5), E12.5, and E16.5 mouse embryos, or of postnatal (day 2) mice, following a published protocol for radioactive *in situ* hybridization (Bulfone *et al.*, 1998). Sets of serial sections were hybridized with ³⁵S-UTP-labeled antisense or sense riboprobes, transcribed from the murine pcDNA-Pc3b vector (corresponding to the region from nt 1 to 1356 in the Pc3b cDNA sequence). The sense probes yielded no hybridization signal.

Flow cytometry assay. The cell cycle profiles were measured as described (Guardavaccaro *et al.*, 2000), with minor modifications. NIH3T3 cells were cotransfected with the murine or human pcDNA3-PC3B construct (or with vector alone) and with a construct encoding the green fluorescent protein (GFP) fused to the cellular membrane protein spectrin (pCMVEGFP-spectrin; Kalejta *et al.*, 1997) by means of the liposome technique, using the Lipofectamine reagent (Life Technologies, Gaithersburg, MD). The cell number at the moment of harvesting (48 h after transfection) was about 1.5 × 10⁶ in a 90-mm dish. The cell cultures were analyzed for cell cycle phase distribution using a FACScan flow cytometer (Becton Dickinson, Franklin Lakes, NJ). Two-color flow cytometry was performed, simultaneously measuring GFP-spectrin (green channel) and propidium iodide (red channel) fluorescence intensities, using CellQuest software with doublet discrimination to remove cell aggregates and debris. The gates to analyze GFP-spectrin/Pc3b-expressing cells were set after the background fluorescence of cells transfected with empty vector was measured. DNA histograms were analyzed using ModFit LT software (Verity Software House Inc., Topsham, ME).

FIG. 1. Nucleotide and predicted amino acid sequence of (A) mouse Pc3b and (B) human PC3B. In each sequence, the ATG start codon and the putative polyadenylation signal are underlined. The translation of the longest ORF is shown above the nucleotide sequence with the single-letter amino acid code. The mouse and human PC3B nucleotide sequences were deposited with the EMBL database under Accession Nos. AJ005120 and AJ271351, respectively. (C) The predicted human and mouse protein sequences are aligned by the algorithm Align.

A Mouse Pc3b

1 GTAGCTGGCTCTCTAACTTTGGACCACCTTTTGTAGAGACAGACGAAATCTTTTGTAGCAAGTGTAATGTGTTTTTATTAACTCTTTTACTGTGCAGTTTTGTAA 103
 1 MRDEIATAVVF 10
 104 GCCACATTTTCCAACGGCGGCTCTGAAGCCTGAATATTGACTCTATGTCTCTACACAGACTGCTTTGGAATCATGAGAGACGAAATGCAACAGCAGTTTTTT 208
 11 FVTRRLVKKHEKLSLSTQQIETFAALKLMTVLF EK YRGH 45
 209 TTTGTACACAAGATTGTTGAAAAGCATGAGAACTGAGTACTCAACAGATAGAAACCTTTGCACTAAAGCTGATGACCGCTTTGTTGAAAAGTACAGAGGTACAC 313
 46 WHPD C P S K G Q A F R C I R I N N N N K D P V L E R A C A E S N 80
 314 TGGCACCCCTGACTGCCCTTCCAAGGGCAGGCTTTTAGGTGTATCAGGATAAACCAACATGAGATAAAGACCCCTGTTTTAGAAAGGGCTGTGTCTGAGAGTAAT 418
 81 V N F F H L G L P K E M T I W V D P Y E V C C R Y G E K K H P F T I A 115
 419 GTGAATTTTTTCACTGGGACTTCCAAAGGAGATGACCATATGGGTGATCCCTATGAGGTGTCTGTAGGTATGGTGAGAAAAAGCATCCCTTTACAAATGGCT 523
 116 S F K G R W E N W E L A Q H V S C A V N R A T G D C S S G T S S D E E 150
 524 TCTTTTAAAGGTAGATGGGAGAACTGGGAGTTGGCTCAGCATGTCAGCTGTGAGTTAACAGAGCCACGGGAGACTGCCTCTGGCACATCTTCTGATGAAGAA 628
 151 S C S R E A Q V I P K V N N P K S V Y Q V E N F K Q S L Q P W F C L P 185
 629 AGCTGCAGCAGGAGGCCAGGTCATCCCAAAGTGAACAACCAAGAGCGCTTACCAGGTGAAAAATTTCAAACAGTCATTCGACCGGTGGTTCTGCTCCCC 733
 186 R R K H L A D G R G F L P G A A C H P V P K S S K W C R P A S R R V D 220
 734 CGTAGAAAAGCATTTGGCAGATGTCGTGGTTCCCTCCCGGGCTGCTGCCACCCAGTCCCAAGAGCTCTAAGTGGTGCCGCGCCAGCTCCGCGCAGGGTGGAC 838
 221 R Y H W V N A Q L F S G Q T A P G E P G E E A L S S L K Q K * 250
 839 AGATATCACTGGTCAACCCCAACTGTTTCACTGGTCAGACAGCACCCAGGAGAGCCTGGAGAAGAGGCTTGTCTTCCCTAAAGCAAAAATGAGGCTAAAGCCAA 943
 944 GAAATGCCCCCACTAGAAAAAATGCCTGCTTCAGAAATGTAGCACAGAAAAGGCTGTCTTGCACACAGACCAGCATTGACTTTTACTACTTTTAAATCTTA 1048
 1049 TTTAACTTTATGTAATAATTTTATGAACACTAGTGAATATAGGTGCCTAGAAAAGTGTAGAACAGAGATGTTGCCCGTGATAAAAATAAAATGAATATAGGAAG 1153
 1154 AAGACTTGAAATAAATCTCTTTGTTTAAACAACTCTAGTTTCTAGTTTGTGCAAGACAGTTTTAAAGTCTGTTTAAATCAITGTTTTTAAAGTAGGTTTTT 1258
 1259 AACTAAGGAAGATTGATCCCTGACAAAATCCCTCTGGACTTGTCTTTTTTTTTTTTTTTTTTTTTTCTTGTAAACAGTCTAATTTTATAAATCTGTTAAAGCTTGG 1363
 1364 TGGAAAAATTTAAGATAAATCCCTTTTATGTCTTTTTAAAGTTTGAATTACAACCTGAAAGTGAATTTACTGATATCATCTATTTTTATAAAGTGGTACT 1468
 1469 TGCTTCTAATAAAGTATTCAAACCTAAGCCCAAAAAAAGAAACCGTTCGACCCGAGCTTTTT 1532

B Human PC3B

1 MRDEIATTVFFVTRRLVKKHDKLSKQIQIEDF 30
 1 GAATCTGAGAGATGAAATGCAACAACAGTTTCTCTTGTACACAAGATTGGTGAAAAACATGATAAACTAAGTAAACAGCAAAATAGAGACTTT 95
 31 AEKLM T I L F E T Y R S H W H S D C P S K G Q A F R C I R I N N N 65
 96 GCAGAAAAGCTGATGCGATCTGTTTGAACAATACAGAAGTCACTGGCAGCTGATTTGCCCTTCTAAAGGGCAAGCCTCAGGTGCAATCAGGATAAAGCAAA 200
 66 Q N K D P I L E R A C V E S N V D F S H L G L P K E M T I W V D P F E 100
 201 CAGAATAAAGATCCCATCTAGAAAAGGCAATGTGTGAAAGTAAATGATGATTTTTCTCACCTGGGACTTCCGAAGGAGATGACCATATGGGTAGATCCCTTTGAA 305
 101 V C C R Y G E K N H P F T V A S F K G R W E E W E L Y Q Q I S Y A V S 135
 306 GTATGCTGTAGTATGGTGAGAAAAACCATCCATTTACAGTTGCTTCTTTTAAAGCCAGATGGGAGGAATGGAACTATATCAACAAATCAGTTATGCAAGTATG 410
 136 R A S S D V S S G T S C D E E S C S K E P R V I P K V S N P K S I Y Q 170
 411 AGAGCCCTCAGAGCTTTCCCTCTGGCCTTCCGCGATGAAGAAAGTTGTAGCAAGGAACCTCGTGTCAATTCCTAAAGTCAGCAATCCGAAGAGTATTTATCAG 515
 171 V E N L K Q P F Q S W L Q I P R K K N V V D G R V G L L G N T Y H G S 205
 516 GTTGAAACTTGAACAGCCCTTTCAATCTGGTTFACAATCCCCGCAAAAAGAAATGGTGGAGCGCGTGTGGCTCCTGGGAAACACTTACCATGGGCTCG 620
 206 Q K H P K C Y R P A M H R L D R I L * 223
 621 CAGAAGCATCTAAGTGTACAGCCCTGCTATGCACCGCTGCAGAGAATTTATAACCCACATCTGGGAATGAATTTGCAGCACCTGCTAGAGAAGGACCCCTT 725
 726 GGAAGGCACTGCCCTGGGCTCCATGGCAGGAAGATGAGAAGAAATCTTACAGGTGATTTCTGGAGCCTGAAAAGAAATAAACAACAAA 814

C

hPC3B MRDEIATTVFFVTRRLVKKHDKLSKQIQIEDFAEKLM 35
 mPc3b MRDEIATAVFFVTRRLVKKHEKLSLSTQQIETFAALKLM 35
 hPC3B TILFETYRSHWHSDCPSKGOAFRCIRINNNQNKDP 70
 mPc3b TVLFEKYRCHWHHPDCPSKGOAFRCIRINNNENKDP 70
 hPC3B ILERACVESNVDFS HLG L P K E M T I W V D F E V C C R Y 105
 mPc3b VLERACAESNVNFFHLGLPKEMTIWVDFYEVCCRY 105
 hPC3B GEKNHPFTVASFKGRWEWEWEL Y Q Q I S Y A V S R A S S D 140
 mPc3b GEK K H P F T I A S F K G R W E N W E L A Q H V S C A V N R A T G D 140
 hPC3B VSSGTSDEEESCSKEPRVIPKVS NPKSIYQVENLK 175
 mPc3b CSSGTSDEEESCSREACVIPKVNPKSVYQVENFK 175
 hPC3B QPFSW L Q I P R K K N V V D G R V G L L G N T Y H G S K H P K 210
 mPc3b QSLQPF C I P R K H L A D G R G F L F G A A C H P V E K S S K 210
 hPC3B CYRPAMHR L D R 221
 mPc3b WCRPASR R V D R Y H W V N A Q L F S G Q T A P G E P G E E A L S 245
 hPC3B IT 223
 mPc3b SIKQK 250

Radiation hybrid mapping. The following primers from the 3' untranslated region of human PC3B were used for direct PCR amplification: 5'-ATCTGGGAATGAATTTGCGACAC-3' (sense primer, corresponding to nt 680–705 of human PC3B sequence); 5'-TCCA-GAAATCACCTGAAGATTTC-3' (antisense primer, corresponding to nt 767–794 of human PC3B sequence). The PCR analysis results were analyzed by the RH Mapping Service of the Whitehead Institute/MIT Center for Genome Research (WICGR) using RH Mapper software. The list of genes involved in genetic disorders mapping at 11q23 was obtained from Online Mendelian Inheritance in Man (OMIM, Center for Medical Genetics, Johns Hopkins University, Baltimore, MD, and National Center for Biotechnology Information, National Library of Medicine, Bethesda, MD).

RESULTS

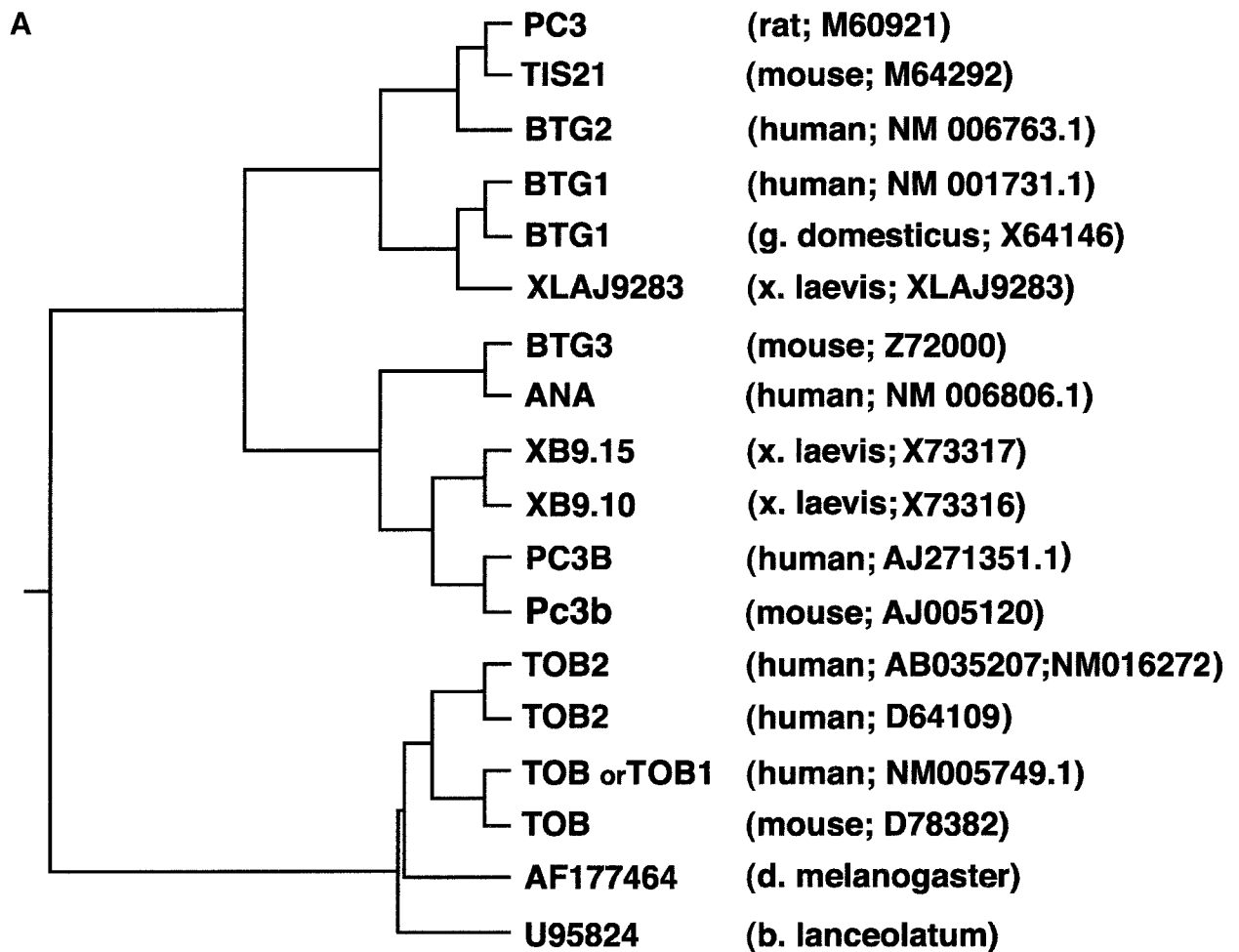
Cloning and Sequencing of Murine and Human PC3B

A portion of the rat PC3 protein sequence corresponding to residues 50–68 was compared to EST databases (dbEST, Boguski *et al.*, 1993) using the TblastN algorithm (Altschul *et al.*, 1990). That region, originally identified as the A box (Guehenneux *et al.*, 1997), is highly conserved throughout the family and was used for database searching, as we recently found it to be necessary for the antiproliferative activity of PC3 (and hence renamed it GR, for growth regulatory; Guardavaccaro *et al.*, 2000). Over 150 ESTs, from either human or murine cDNA libraries at different stages of development (October 1997), showed homology with the GR query sequence. Of those, about 20 ESTs with significant homology to known genes of the PC3/BTG/TOB family, yet not identical to any of them, were considered for further analysis. Sequence analysis was then carried out on cDNA clone 944385 (isolated from a murine 2-cell stage embryo cDNA library; WashU-HHMI Mouse EST Project), corresponding to mouse EST AA545570. Clone 944385, named Pc3b, has a cDNA insert of about 1450 nt that contains the entire coding region. The first in-frame ATG is located 178 nt from the 5' end of the clone and fulfills Kozak's criteria for an initiation codon (Kozak, 1984). Comparison of the complete sequence of clone 944385 with dbEST indicated the presence of several ESTs belonging to the same transcriptional unit, 3 of them further extending the UTR 5' end by about 80 nt. These ESTs were assembled to obtain the complete sequence of mouse Pc3b cDNA, which has a total length of 1532 nt, with a 5' UTR of 178 nt and a 3' UTR of 604 nt (Fig. 1A). The predicted protein product encoded by the ORF is 250 residues long (Fig. 1A) with a calculated molecular mass of 28,588 Da. The murine Pc3b sequence was then used as a query to retrieve its human counterpart in the EST database. This led to the identification of 3 human ESTs, part of the same transcriptional unit, with a high level of homology to mouse Pc3b. Sequence analysis of the corresponding cDNA clones (clones 1583867, 2347887, and 2350245, corresponding to ESTs AA972143, AI798233, and AI827608, respectively) yielded the full sequence of the putative human PC3B cDNA, 814 nt in size, with a predicted protein

product of 223 residues and a calculated molecular mass of 25,973 Da (Fig. 1B). Sequence inspection using the program Prosite (Bairoch, 1990) showed potential phosphorylation sites by protein kinase C, of which only one at Ser-116 is conserved in human and mouse PC3B sequences, and potential phosphorylation sites by casein kinase II (those conserved are at aa 145–148 and 146–149). No consensus site for phosphorylation by CDK2 was detected (which is present and functional in PC3; Guardavaccaro *et al.*, 2000).

PC3B, A Novel Member of the PC3/BTG/TOB Gene Family

Mouse Pc3b cDNA-deduced protein, when compared to the GenBank, EMBL, DDBJ and PDB databases using the algorithm TblastN (March 2000), presented the highest level of homology to human PC3B protein (*E* value of 5×10^{-86}), with an identity of 73.09% based on alignment by the algorithm Align (Feng and Doolittle, 1996), followed by two sequences from *Xenopus*, i.e., XB9.10 and XB9.15 (*E* values of 2×10^{-59} and 4×10^{-58} with 47.8 and 48.9% identity, respectively; see also Figs. 1B and 2B). The next protein sequences showing a near level of identity with mouse PC3B protein followed at some distance; these were rat and mouse BTG3 (Guehenneux *et al.*, 1997; the latter protein is alternatively termed mouse ANA; see Yoshida *et al.*, 1998), human ANA (Yoshida *et al.*, 1998), and PC3 (Bradbury *et al.*, 1991). These four genes presented 39.2, 39.2, 38.4, and 33.1% identity, respectively, to mouse PC3B protein (Figs. 2B and 3). The human PC3B cDNA-deduced protein shared with the mouse PC3B protein the same level of homology for the XB9.10, XB9.15, BTG3/ANA, and PC3 genes (see Fig. 2B). Therefore, these data (i) suggest that the cDNA identified as human PC3B is the homologue of mouse Pc3b cDNA and (ii) clearly indicate that murine/human PC3B is significantly correlated with the PC3/BTG/TOB gene family, but is not identical to any of those genes. To clarify further the correlation of PC3B with the genes of the family, we generated a phylogenetic tree using the algorithms Align and Treedraw by Feng and Doolittle (1996; Figs. 2A and 2B). We analyzed all protein sequences that presented a significant correlation with PC3B (March 2000), as identified by means of the algorithm TblastN within the databases indicated above. This confirmed that PC3B is a novel member of a family comprising so far eight different genes, as shown in Fig. 2: (1) human BTG1/*Gallus domesticus* BTG1 (rat BTG1 and mouse BTG1 are not indicated, being reported in database as identical to human BTG1); (2) rat PC3/mouse TIS21/human BTG2; (3) mouse BTG3/human ANA (rat BTG3 sequence was not reported as it was very similar to mouse BTG3); (4) mouse Pc3b/human PC3B and *Xenopus* B9.10; (5) *Xenopus* XB9.15; (6) human TOB/mouse TOB; (7) human TOB2 (Ikematsu *et al.*, 1999, Accession No. D64109, previously known as TOB4); (8) human TOB2 (similar



B

	hBTG1	XLA	TIS21	PC3	BTG2	mBTG3	hANA	XB9.15	XB9.10	mPc3b	hPC3B	hTOB	mTOB	hTOB2*	hTOB2
hBTG1	0.00	78.11	65.19	64.56	66.46	37.11	35.85	30.82	29.56	32.70	29.56	38.36	37.74	33.96	32.70
XLA	78.11	0.00	61.15	62.42	60.51	38.61	37.97	32.91	31.01	32.28	27.22	35.44	34.81	32.28	31.01
TIS21	65.19	61.15	0.00	97.47	93.67	36.49	37.16	33.11	33.11	32.43	30.41	35.81	35.14	33.11	33.78
PC3	64.56	62.42	97.47	0.00	92.41	37.16	37.84	33.78	33.78	33.11	31.08	35.81	35.14	33.78	34.46
BTG2	66.46	60.51	93.67	92.41	0.00	36.49	36.49	32.43	32.43	33.78	31.76	36.49	35.81	33.11	33.78
mBTG3	37.11	38.61	36.49	37.16	36.49	0.00	93.25	46.35	45.57	39.27	44.84	24.60	26.21	23.79	24.19
hANA	35.85	37.97	37.16	37.84	36.49	93.25	0.00	45.92	45.15	38.46	43.95	22.18	23.79	21.37	21.37
XB9.15	30.82	32.91	33.11	33.78	32.43	46.35	45.92	0.00	90.48	48.93	55.66	23.58	22.71	21.83	20.52
XB9.10	29.56	31.01	33.11	33.78	32.43	45.57	45.15	90.48	0.00	47.88	55.41	24.03	21.89	21.03	20.17
mPc3b	32.70	32.28	32.43	33.11	33.78	39.27	38.46	48.93	47.88	0.00	73.09	23.17	22.76	21.54	20.73
hPC3B	29.56	27.22	30.41	31.08	31.76	44.84	43.95	55.66	55.41	73.09	0.00	21.92	21.92	20.18	20.18
hTOB	38.36	35.44	35.81	35.81	36.49	24.60	22.18	23.58	24.03	23.17	21.92	0.00	93.91	53.89	50.30
mTOB	37.74	34.81	35.14	35.14	35.81	26.21	23.79	22.71	21.89	22.76	21.92	93.91	0.00	52.94	49.41
hTOB2*	33.96	32.28	33.11	33.78	33.11	23.79	21.37	21.83	21.03	21.54	20.18	53.89	52.94	0.00	87.79
hTOB2	32.70	31.01	33.78	34.46	33.78	24.19	21.37	20.52	20.17	20.73	20.18	50.30	49.41	87.79	0.00

FIG. 2. Phylogenetic relationship in the PC3/BTG/Tob family. **(A)** The sequences significantly correlated with PC3B were identified by the TblastN algorithm analyzing the GenBank, EMBL, DDBJ, and PDB databases combined (December 1, 1999), and then an evolutionary tree was calculated with the nearest-neighbor algorithm by Feng and Doolittle (1996). The evolutionary distance is shown by the total branch lengths (horizontal lines). The accession numbers of the genes reported are also indicated, whereas their existing references and alternative accession numbers are as follows: human BTG1, NM 01731.1 or, alternatively, X61123.1 (Rouault *et al.*, 1992); *G. domesticus* BTG1, X64146 (Rouault *et al.*, 1993); TIS21, M64292 or, alternatively, NM007570.1 (Fletcher *et al.*, 1991); PC3, M60921 (Bradbury *et al.*, 1991); BTG2, NM 006763.1 or, alternatively, U72649.1 (Rouault *et al.*, 1996); mouse BTG3, Z72000 or, alternatively, NM009770.1 (Guehenneux *et al.*, 1997), cloned also as mouse ANA, D83745 (Yoshida *et al.*, 1998); human ANA, NM006806.1 or, alternatively, D64110.1 (Yoshida *et al.*, 1998); human PC3B, AJ271351; mouse Pc3b, AJ005120 (present report); human TOB1, NM 005749.1 (previously named TOB with Accession No. D38305.1, Matsuda *et al.*, 1996); human TOB2 (as by Ikematsu *et al.*, 1999; Accession No. D64109, previously known as TOB4). The remaining sequences are present (March 2000) only in the database (rat BTG1, L26268; XLAJ9283; rat BTG3, AF087037; XB9.15, X73317; XB9.10, X73316; mouse TOB, D78382 or, alternatively, NM009427.1; human TOB2, AB035207 or, alternatively, NM016272). Rat BTG1 (L26268) and mouse BTG1 (L16846 or Z16410; Rouault *et al.*, 1993), were not reported in the phylogenetic tree since their sequence in the database was identical to that of human BTG1. **(B)** Percentage identities between the proteins analyzed. Human TOB2 (AB035207) is indicated with an asterisk to differentiate it from TOB2 (D64109). The alignment used was that indicated in **(A)** to implement the phylogenetic tree.

		Box A	Box B	
hBTG1	40	F SQSLQELLAEHYKHHWFPEK PCKGSGYRC IRIN--HKMDPLIGQAAQRIGLSSQELFRL LPSELTLWVDPYEV SYRIGEDG SGICVL		124
mBTG1	40	F SQSLQELLAEHYKHHWFPEK PCKGSGYRC IRIN--HKMDPLIGQAAQRIGLSSQELFRL LPSELTLWVDPYEV SYRIGEDG SGICVL		124
rBTG1	40	F SQSLQELLAEHYKHHWFPEK PCKGSGYRC IRIN--HKMDPLIGQAAQRIGLSSQELFRL LPSELTLWVDPYEV SYRIGEDG SGICVL		124
bBTG1	40	F SQSLQELLAEHYKHHWFPEK PCKGSGYRC IRIN--HKMDPLIGQAAQRIGLSSQELFRL LPSELTLWVDPYEV SYRIGEDG SGICVL		124
gBTG1	40	F SQSLQELLAEHYKHHWFPEK PCKGSGYRC IRIN--HKMDPLIGQAAQRIGLSSQELFRL LPSELTLWVDPYEV SYRIGEDG SGICVL		124
XLA	39	F NQSLQDLLADHYKHHWFPEK PTKGSAYRC IRIN--HKMDPLIGQAADRIGLNSQQMFQL LPSELTLWVDPYEV SYRIGEDG SGICVL		123
TIS21	38	F SRALQDALTDHYKHHWFPEK PSKGSYRC IRIN--HKMDPIISKVASQIGLSPQLHRL LPSELTLWVDPYEV SYRIGEDG SGICVL		122
PC3	38	F SRALQDALTDHYKHHWFPEK PSKGSYRC IRIN--HKMDPIISKVASQIGLSPQLHRL LPSELTLWVDPYEV SYRIGEDG SGICVL		122
BTG2	38	F SGALQDALTEHYKHHWFPEK PSKGSYRC IRIN--HKMDPIISKVASQIGLSPQLHRL LPSELTLWVDPYEV SYRIGEDG SGICVL		122
rBTG3	30	F AEKLTQILQEYKKNHWYEPK PSKGQAYRC IRVKNFQRVDPDLKACEDSCILYSDL-- GLPKELTLWVDPCEVCCRYGKKNNAFIV		114
mBTG3	30	F AEKLTQILQEYKKNHWYEPK PSKGQAYRC IRVKNFQRVDPDLKACENSCILYSDL-- GLPKELTLWVDPCEVCCRYGKKNNAFIV		114
MANA	30	F AEKLTQILQEYKKNHWYEPK PSKGQAYRC IRVKNFQRVDPDLKACENSCILYSDL-- GLPKELTLWVDPCEVCCRYGKKNNAFI		114
hANA	30	F AEKLTQILQEYKKNHWYEPK PSKGQAYRC IRVKNFQRVDPDLKACENSCILYSDL-- GLPKELTLWVDPCEVCCRYGKKNNAFIV		114
xB9.15	30	F AAKLTTLFAKYKTHWYAEN PTKGQAFRC IRINECQALDAVLEKACTESNVDFNEL-- GLPKEMTIWVDPFEVCCRYGKKNDFPTI		114
xB9.10	30	F AAKLTTLFAKYKKNHWYAEN PMKGQAFRC IRINTYQALDAVFEKACAESNVDFNDL-- GLPKEMTIWVDPFEVCCRYGKKNDFPTI		114
hPC3B	30	F AEKLTQILQEYKKNHWYEPK PSKGQAFRC IRINNNKDPILERACVESNVDFSHL-- GLPKEMTIWVDPFEVCCRYGKKNHPFTV		114
mPc3b	30	F AEKLTQILQEYKKNHWYEPK PSKGQAFRC IRINNNKDPVLERACAESNVDFPHL-- GLPKEMTIWVDPFEVCCRYGKKNHPFTI		114
hTOB	28	F GEELERLLKKKYEGHWYEPK PKGSGFR CIHIG--EKVDPVIEQASKESGLDIDDVRGNL PQDLSVWIDPFEV SYQIGEK GPVKVL		112
mTOB	28	F GEELERLLKKKYEGHWYEPK PKGSGFR CIHVG--EKVDPVIEQASKESGLDIDDVRGNL PQDLSVWIDPFEV SYQIGEK GPVKVL		112
hTOB2*	28	F GEELERLLKKKYEGHWYEPK PLKGSFR CVHIG--EMVDPVVELAAKRSGLAVEDVRAN PEELSVWIDPFEV SYQIGEK GAVKVL		112
hTOB2	28	F GEELERLLKKKYEGHWYEPK PLKGSFR CVHIG--EMVDPVVELAAKRSGLAVEDVRAN PEELSVWIDPFEV SYQIGEK GAVKVL		112
BLA	28	F AALAKGLLAKFEGHWYEPK PKGSGYRC IRIS--TTLDPVVLKACDASGLDITDVKGHL PEELSIWVDPKEV SYRMGER GPVKIL		112
DME	24	F GEELERLLRDKFQDHWYEPK PKGSAYRC LKIG--DPIDSVLERAARESGVPIGDILENL PNELSVWIDPGEV SFRIGEK GAVKIL		108
<div style="display: flex; justify-content: space-around; margin-top: 10px;"> Y H P SGY N A S L ELT V S R </div> <div style="display: flex; justify-content: space-around; margin-top: 5px;"> F---L---L--- --W- --P-KG RCI---D-----P- -W DP-EV - -GE----- </div> <div style="display: flex; justify-content: space-around; margin-top: 5px;"> F P A QAF G V I V DMS I C Q </div>				

FIG. 3. Conserved regions within the BTG/PC3/TIS/TOB family. Multiple comparisons between the mouse/human PC3B deduced amino acid sequence and the proteins significantly correlated with it (identified and aligned as described in the legend to Figs. 2A and 2B and under Results) pointed out the existence of two regions of higher homology, termed the A and B boxes. The amino acids conserved throughout all the different protein sequences (or in the majority of them) are in boldface type. Nomenclature is the same as in Fig. 2, with the addition of a prefix to protein names where necessary: h, human; m, mouse; r, rat; b, *Bos taurus*; g, *Gallus domesticus*; x, *Xenopus*. XLA, Accession No. XLAJ9283; BLA, Accession No. U95824; DME, Accession No. AF177464.

to D64109, present only in database with Accession Nos. AB035207 and NM016272). Furthermore, the gene products identified in *Drosophila melanogaster* and *Branchiostoma lanceolatum* with Accession Nos. AF1774464 and U95824, respectively, also appear to be TOB-related genes (see Fig. 2).

Furthermore, the multiple comparisons performed by the algorithm Align, between the known members of the PC3/BTG/TOB gene family, confirmed the existence of two domains of higher conservation, corresponding to the A—or GR—and B boxes that are also shared by the PC3B protein (Fig. 3). Such conserved regions correspond within the mouse and human PC3B proteins to residues 42–60 and 88–107 (aa 50–68 and 96–115 in rat PC3); see Fig. 3.

Expression of PC3B in Germline, Adult, and Embryonic Tissues

To analyze PC3B gene expression, the mouse 944385 and human 2347887 cDNA clones were ³²P-labeled and used to probe Northern blots of poly(A)⁺ mRNA from mouse and human adult tissues, respectively (Figs. 4A, 4C, and 4D). A specific signal was detected only in testis, visualizing a 1.4-kb-long mRNA transcript in both the murine and the human panels. Given that the ESTs belonging to the same transcriptional unit of mouse and human PC3B cDNAs had been isolated from libraries of testis, as well as of oocyte and of early preimplantation embryos (2- or 8-cell stages; March 2000), we sought to define in the latter two tissues the

expression of murine Pc3b mRNA. By RT-PCR we observed that Pc3b mRNA was highly expressed in oocyte, with a progressive decrease as the embryo reached the morula stage (about 16 cells) and blastocyst stage (about 64 cells, Fig. 4B). Indeed, the expression of mouse Pc3b, analyzed by densitometry and normalized to that of β -actin, declined, with respect to the expression observed in oocyte assumed as unity, to 0.7-fold in morula and to 0.3-fold in the blastocyst.

Expression of Mouse PC3B during Development

To determine the temporal and spatial expression of Pc3b during mouse development, an RNA *in situ* expression study was performed on mouse embryo tissue sections at several developmental stages, from E10.5 to E16.5 and at P2 (postnatal day 2). A 1.4-kb-long RNA probe was produced by the pcDNA-Pc3b vector 3'UTR-less. The earliest Pc3b expression was detected at around E16.5. At this time point, Pc3b is expressed exclusively in the epithelium of the nasal cavity (Figs. 5A–5D). No expression was detected in P2 animals. The sense strand of the same fragments did not reveal any detectable signal above the background level (data not shown).

In rodents, most of the surface area of the nasal cavities is covered with olfactory mucosa. The olfactory neuroepithelium (OE) is composed of three major cellular components: the supporting (sustentacular) cells that form a single layer close to the surface; the sensory olfactory receptor neurons (ORN), occupying the lower two-

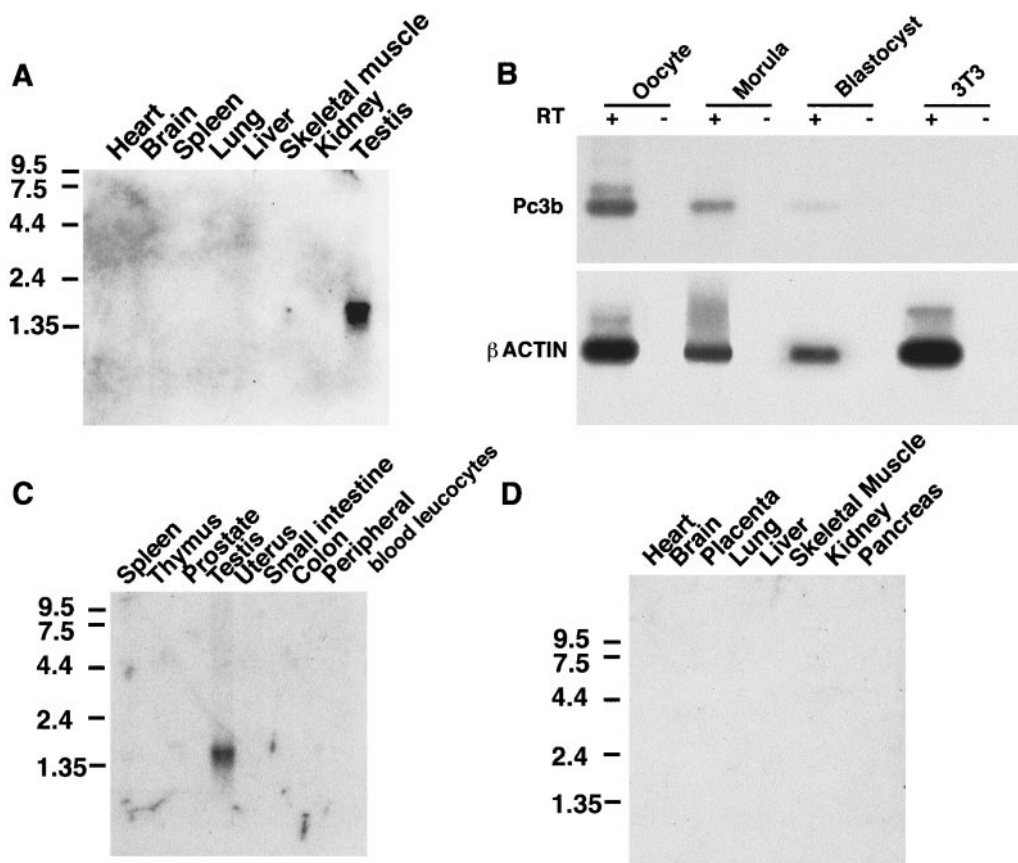


FIG. 4. Expression of PC3B in adult and germline tissues. (A) The blot contained 2 μ g of poly(A)⁺ RNA/lane, obtained from eight different mouse tissues. The filter was hybridized with the mouse Pc3b clone. (B) The murine mRNA species indicated were quantified by RT-PCR analysis. Equal amounts of the RT-PCR products amplified were blotted on filters and visualized using specific primers (see Materials and Methods). RT+ or - indicates the products of amplification performed in parallel on two aliquots of each RNA starting sample preincubated or not with RT, to check for the presence of DNA contamination. Control amplifications using as template the cDNA corresponding to each mRNA species gave a signal of the expected size (not shown). (C) and (D) The blot contained 2 μ g of human poly(A)⁺ RNA/lane, from the indicated tissues. The filter was hybridized with the human PC3B clone. Control hybridizations of Northern blots in (A), (C), and (D) with a β -actin cDNA probe indicated the presence of approximately equal amounts of RNA in all lanes (data not shown).

thirds of the epithelium; and the globose basal cells along the basement membrane, which represent the neuronal precursors that become postmitotic neurons immediately after a few symmetric divisions (Graziadei and Monti-Graziadei, 1979; Calof and Chikaraishi, 1989; Schwartz Levey *et al.*, 1991; Calof *et al.*, 1996). Our *in situ* experiments showed that Pc3b is not expressed in the most dorsal and medial areas in this structure at this stage, while it is intensely expressed in the remaining olfactory and respiratory epithelium (Figs. 5A–5D). Moreover, the transcript seems to be preferentially distributed in the luminal half of the epithelium where the most mature postmitotic cells are located (Fig. 5B). Therefore the Pc3b spatial and temporal pattern of expression suggests that it is expressed in the supporting cells and possibly in the sensory neurons, while the immature olfactory neurons (globose basal cells) are negative.

Analysis of the Antiproliferative Activity of PC3B

Given the established antiproliferative effects of many members of the PC3/BTG/TOB gene family, we sought to

verify whether PC3B was also able to inhibit cell proliferation, by measuring the cell cycle profile of NIH3T3 cells expressing ectopic PC3B. With this aim we cotransfected the pcDNA-PC3B (either murine or human) expression construct together with a vector expressing GFP-spectrin (Kalejta *et al.*, 1997). Successfully transfected cells were revealed by GFP-spectrin expression and analyzed for their cell cycle profile by two-color flow cytometry (Figs. 6A and 6B). The analysis was carried out on the whole cell population transfected, i.e., both floating and adherent cells. The former were included to detect whether PC3B induced cellular death. We observed that the expression of murine (Figs. 6A and 6B) and human (data not shown) PC3B in NIH3T3 cells induced an evident increase of the cell population in the G₁ phase, paralleled by a complementary decrease of cells in the S and G₂/M phases. Ectopic PC3B did not affect the size of the hypodiploid sub-G₁ population, which corresponds to the fraction of cells undergoing apoptosis (Hotz *et al.*, 1994; Figs. 6A and 6B). This indicated that the inhibition of cell cycle progression is not due to no-specific

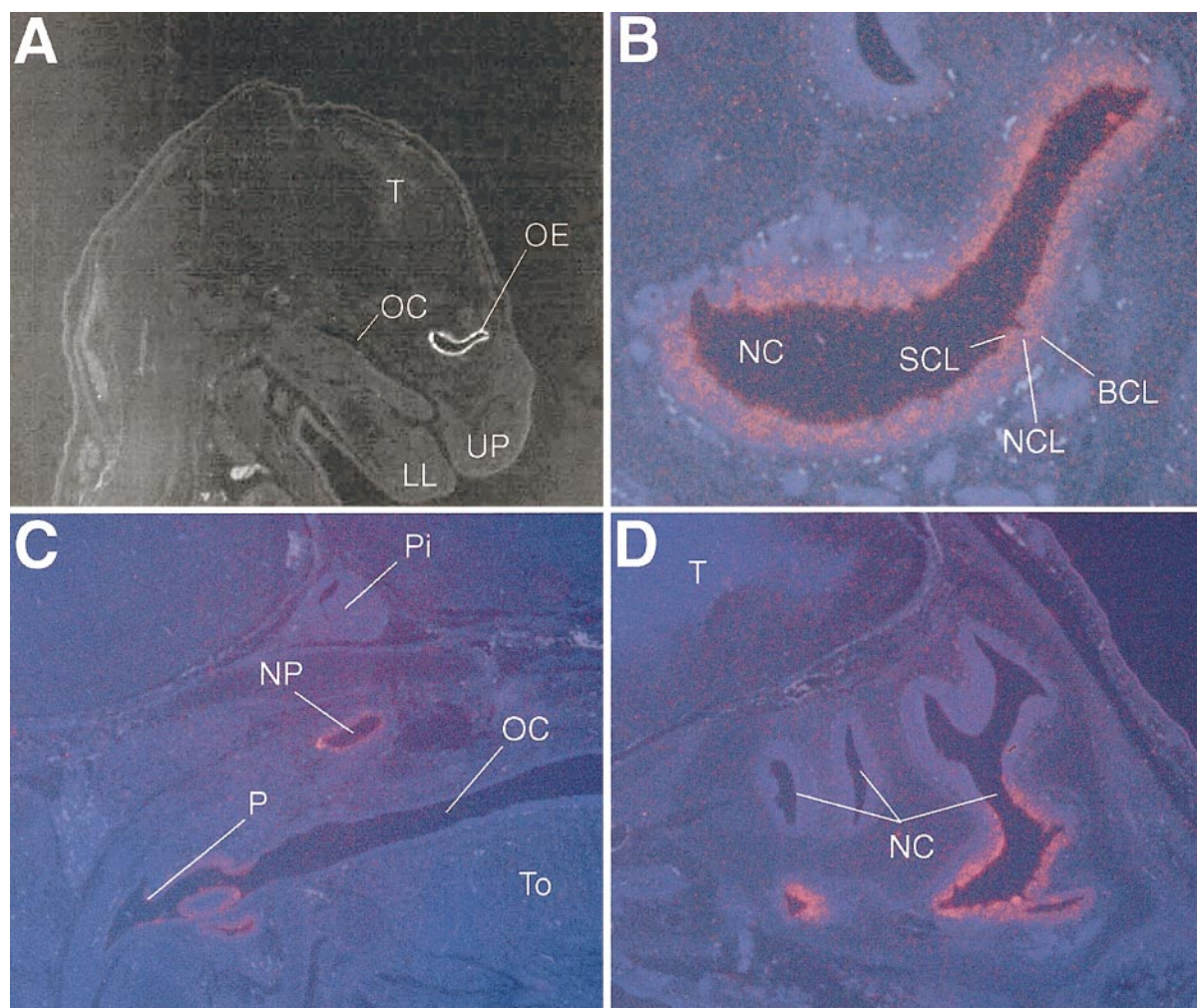


FIG. 5. RNA *in situ* hybridization on E16.5 mouse tissue sections. As shown in **A**, and at higher magnification in **B**, Pc3b is expressed exclusively in the nasal epithelium. The hybridization signal (in red in **B–D**) is more intense in the inner layers of the epithelium: sustentacular and neuronal cell layers. The transcript could not be detected in the more dorsal and medial areas of the nasal cavities, as shown in **D**. Pc3b is instead expressed, at a lower level, in the epithelium of the naso- and oropharynx, as shown in **C**. SCL, sustentacular cell layer; NCL, neuronal cell layer; BCL, basal cell layer; OC, oral cavity; NC, nasal cavity; P, pharynx; Pi, pituitary; NP, nasopharynx; OE, olfactory epithelium; LL, lower lip; UP, upper lip; T, telencephalon.

effects, such as cellular toxicity of the transfected DNA. As an independent approach, inhibition of proliferation by murine pcDNA-Pc3b was also assessed, and confirmed, by colony formation assay, performed as described (Guardavaccaro *et al.*, 2000; data not shown).

Chromosomal Localization of the PC3B Locus

RH mapping (Cox *et al.*, 1990) was used to determine the chromosomal band position of the PC3B gene. RH mapping was performed using the GeneBridge 4 panel (Walter *et al.*, 1994), which includes 93 human/hamster clones. RH mapping indicated a univocal localization to chromosome 11 between the markers WI-6355 and WI-7642. These markers are localized to the cytogenetic band 11q23.2–q3, as reported by Chumakov *et al.* (1995). To evaluate a possible involvement of this gene in human inherited disorders, we used the OMIM database. We retrieved

information on the disease loci mapped to the same chromosomal region, which comprises different types of myeloid and lymphoid leukemias associated with breakpoint regions, paragangliomas, and different variants of the ataxia–telengectasia syndrome.

DISCUSSION

We report here the isolation of murine Pc3b cDNA and of its human homologue, on the basis of its similarity to the GR region of the PC3 gene, which is conserved within the PC3/BTG/TOB protein family and is necessary for the antiproliferative activity of PC3 (Guardavaccaro *et al.*, 2000). Our analyses show that the PC3B cDNA encodes a novel protein of the family, very likely the homologue of either the *Xenopus* B9.10 or B9.15 gene. The phylogenetic tree generated with the protein sequences of the whole gene family reveals three major clusters, one comprising two genes,

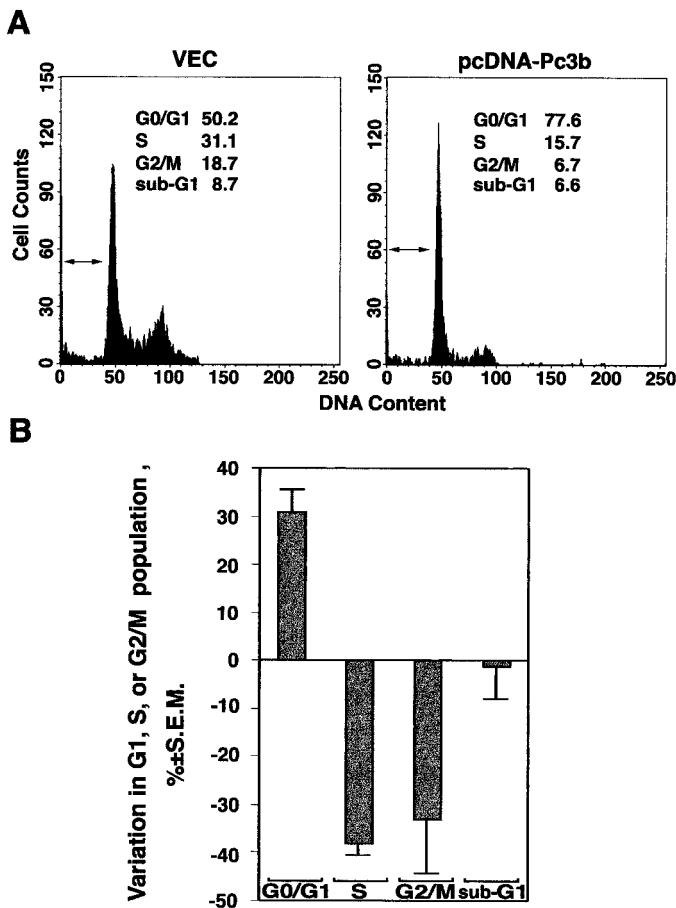


FIG. 6. Effects of PC3B on the proliferation rate of NIH3T3 cells. (A) Flow cytometry analysis of the effects of mouse Pc3b on the cell cycle profile in NIH3T3 cells, from a representative experiment. The percentages of cells in G₁, S, G₂/M, and sub-G₁ (indicated by the double-headed arrow) phases of the cell cycle are reported. About 3×10^5 NIH3T3 cells were seeded onto 90-mm culture dishes, and after 24 h, the cells were transfected either with pcDNA3 empty plasmid (8.5 μ g) or with pcDNA-Pc3b (8.5 μ g), together with a plasmid encoding the GFP-spectrin cell surface marker (pCMVE GFP-spectrin, 1.5 μ g). After 48 h, the transfected cells were harvested and analyzed by means of a FACScan flow cytometer. The cell cycle distribution of GFP-positive cells was measured by analyzing the DNA content after staining with propidium iodide, using two-color flow cytometry. (B) Statistical analysis of the effects of mouse Pc3b on the cell cycle profile. Data from three independent experiments, performed and analyzed as described in (C), are shown as means \pm SEM of the changes in the percentage of cells in G₀/G₁, S, G₂/M, or sub-G₁ cycle phases, referred to the corresponding value of the control transfection with the empty vector pcDNA3.

i.e., BTG1 and PC3/BTG2/TIS21; a second including the genes PC3B/XB9.10, or PC3B/XB9.15, and BTG3/ANA; and a third and more distant cluster composed of at least three genes, TOB, and the two human TOB2 (plus the *D. melanogaster* and *B. lanceolatum* sequences that are part of this third cluster; see legend to Fig. 2 for accession numbers and references). This analysis confirms the indication obtained with the Blast algorithm, that the nearest neighbors of PC3B, in terms of evolutionary distance, are the genes XB9.15, XB9.10, BTG3/ANA, and PC3/BTG2/TIS21. It is worth

noting that the last two genes have a common pattern of expression in the ventricular area of the neural tube (Guehenneux *et al.*, 1997), which suggests a common function.

The expression of PC3B appears to be rather peculiar, being selectively limited to the olfactory epithelium and to germline tissues, including testis and oocyte. This is based on our Northern analysis data, and on the evidence that the ESTs belonging to the same transcriptional unit of PC3B (murine or human) are all, so far, from libraries made from testis, from oocyte, and from 2- to 8-cell embryos. Furthermore, the observation of an absolute decrease of the PC3B mRNA throughout the late cleavages of the oocyte with a rate only slightly greater than that of β -actin, which is actively synthesized during oogenesis and in cleavage-stage embryos in mice (Taylor and Piko, 1990), leaves open the possibility that PC3B is actively synthesized during the maturation of the embryo, rather than being merely of maternal origin. It is worth noting that germline cells are totipotent, in the sense that by differentiation into haploid gametes and fertilization they are able to generate a new organism (see for review, Pesce *et al.*, 1998, and Eyal-Giladi, 1997). As the embryo blastomeres divide, there is a restriction of potency; intriguingly, this process is paralleled by a decrease in the expression of PC3B. At any rate, the high-level expression of PC3B in oocyte as well as in testis (although currently we do not know which cellular population of that organ is responsible for the expression of PC3B) strongly suggests that PC3B might have a role in gametogenesis.

The OE, where Pc3b is also highly expressed, is another tissue peculiar for its conservation of the growth potential. Situated within the nasal cavity, the OE constantly regenerates neurons throughout the lifetime of animals, including rodents and humans (Moulton, 1974; Graziadei and Monti-Graziadei, 1978, 1979; Suzuki and Takeda, 1993). This is a unique feature in the nervous system, which indicates that neuronal stem cells are preserved in the OE throughout life (Graziadei and Monti-Graziadei, 1978). In the rat, each olfactory receptor neuron degenerates every 4–6 weeks and is replaced by a newly differentiated precursor neuron, which is initially located in the basal region of the OE and progressively assumes a mature state of postmitotic neuron while migrating to the upper layers, to finally project afferent axons directly back into the olfactory bulb (Farbman, 1990). Therefore, a gradient of undifferentiated to differentiated cells occurs from the basal to the apical regions of the OE.

The OE becomes arranged in layers (see Results) at around E13, and the differentiation of the sustentacular cells starts at about E15.5, and their nuclei remain confined to the luminal side (Smart, 1971; Cuschieri and Bannister, 1975). The expression of Pc3b in the intermediate and luminal region of the OE, at E16.5, corresponds to the region and time at which the postmitotic neurons localize in the median region of the

epithelium and the sustentacular cells differentiate. Given the ability of Pc3b to induce an impairment of the cell cycle in G₁ phase, it is possible that Pc3b might be involved in the process of differentiation of either the sustentacular cells or the ORN cells, or both, by regulating the growth arrest that precludes and accompanies differentiation. Certainly, further studies in neuronal cells will be helpful in clarifying this possibility.

Very little is known about the genes that regulate proliferation and differentiation of the OE. So far, it has been shown that Mash1, expressed from E10 to E17, is necessary for the generation of the majority of ORN cells (Cau *et al.*, 1997). Two other genes are expressed in the OE, i.e., Math4C and NeuroD, at E10 and E17, respectively. The expression of these three genes follows a basal to apical gradient, with Mash1 being only basal, Math4C being basal and intermediate, and NeuroD being intermediate and apical (Cau *et al.*, 1997). Hence, NeuroD expression is related to the most differentiated ORN, being concomitant with the last division of ORN progenitors and the beginning of differentiation of postmitotic neurons. From our data, PC3B expression is more similar to that of NeuroD, spatially and also temporally, being undetectable until E16, thus partially overlapping the stage of differentiation marked by NeuroD.

Further functional analyses, *in vitro* as well as *in vivo* and in animal models, will be helpful in verifying the functional hypotheses presented in this report. These include the possibility that alterations of the PC3B gene, a cell cycle inhibitor localized at 11q23, might play a part in the onset of one of the different tumor diseases mapping to this chromosomal region.

ACKNOWLEDGMENTS

We are grateful to Richard Butler for installing the Align software in our computer system, to Giuseppe Borsani for his scientific advice, and to Sergio Cattadori for technical support. This work was supported by the Maria Bianchi grant to F.T.

REFERENCES

- Altschul, S. F., Gish, W., Miller, W., Myers, E. W., and Lipman, D. J. (1990). Basic local alignment search tool. *J. Mol. Biol.* **215**: 403–410.
- Bairoch, A. (1990). "Dictionary of Protein Size and Patterns," Ph.D. thesis, Université de Genève.
- Boguski, M. S., Lowe, T. M., and Tolstoshev, C. M. (1993). dbEST—Database for "expressed sequence tags." *Nat. Genet.* **4**: 332–333.
- Bradbury, A., Possenti, R., Shooter, E. M., and Tirone, F. (1991). Molecular cloning of PC3, a putatively secreted protein whose mRNA is induced by nerve growth factor and depolarization. *Proc. Natl. Acad. Sci. USA* **88**: 3353–3357.
- Buanne, P., Incerti, B., Guardavaccaro, D., Avvantaggiato, V., Simone, A., and Tirone, F. (1998). Cloning of the human interferon-related developmental regulator (IFRD1) gene coding for the PC4 protein, member of a novel family of developmentally regulated genes. *Genomics* **51**: 233–242.
- Bulfone, A., Gattuso, C., Marchitello, A., Pardini, C., Boncinelli, E., Borsani, G., Banfi, S., and Ballabio, A. (1998). The embryonic expression pattern of 40 murine cDNAs homologous to *Drosophila* mutant genes (Dres): A comparative and topographic approach to predict gene function. *Hum. Mol. Genet.* **7**: 1997–2006.
- Calof, A. L., and Chikaraishi, D. M. (1989). Analysis of neurogenesis in a mammalian neuroepithelium: Proliferation and differentiation of an olfactory neuron precursor *in vitro*. *Neuron* **3**: 115–127.
- Calof, A. L., Hagiwara, N., Holcomb, J. D., Mumm, J. S., and Shou, J. (1996). Neurogenesis and cell death in olfactory epithelium. *J. Neurobiol.* **30**: 67–81.
- Cau, E., Gradwohl, G., Fode, C., and Guillemot, F. (1997). Mash1 activates a cascade of bHLH regulators in olfactory neuron progenitors. *Development* **124**: 1611–1621.
- Chumakov, I. M., Rigault, P., Le Gall, I., Bellanné-Chantelot, C., Billault, A., Guillou, S., Soularue, P., Guasconi, G., Poullier, E., Gros, I., *et al.* (1995). A YAC contig map of the human genome. *Nature* **377**: 175–297.
- Cox, D. R., Burmeister, M., Price, E. R., Kim, S., and Myers, R. M. (1990). Radiation hybrid mapping: A somatic cell genetic method for constructing high resolution maps of mammalian chromosomes. *Science* **250**: 245–250.
- Cuschieri, A., and Bannister, L. H. (1975). The development of the olfactory mucosa in the mouse: Light microscopy. *J. Anat.* **119**: 277–286.
- Eyal-Giladi, H. (1997). Establishment of the axis in chordates: Facts and speculations. *Development* **124**: 2285–2296.
- Farbman, A. I. (1990). Olfactory neurogenesis: Genetic or environmental control? *Trends Neurosci.* **13**: 362–365.
- Feinberg, A. P., and Vogelstein, B. (1983). A technique for radiolabeling DNA restriction endonuclease fragments to high specific activity. *Anal. Biochem.* **132**: 6–13.
- Feng, D. F., and Doolittle, R. F. (1996). Progressive alignment of amino acid sequences and the construction of phylogenetic trees from them. *Methods Enzymol.* **266**: 368–382.
- Fletcher, B. S., Lim, R. W., Varnum, B. C., Kujubu, D. A., Koski, R. A., and Herschman, H. R. (1991). Structure and expression of TIS21, a primary response gene induced by growth factors and tumor promoters. *J. Biol. Chem.* **266**: 14511–14518.
- Graziadei, P. P. C., and Monti-Graziadei, G. A. (1978). Continuous nerve cell renewal in the olfactory system. In "Handbook of Sensory Physiology" (M. Jacobson Ed.), Vol. IX, pp. 55–82, Springer Verlag, Berlin.
- Graziadei, P. P. C., and Monti-Graziadei, G. A. (1979). Neurogenesis and neuron regeneration in the olfactory system of mammals. I. Morphological aspects of differentiation and structural organization of the olfactory sensory neurons. *J. Neurocytol.* **8**: 1–18.
- Guardavaccaro, D., Corrente, G., Covone, F., Micheli, L., D'Agnano, I., Starace, G., Caruso, M., and Tirone, F. (2000). Arrest of G₁-S progression by the p53-inducible gene PC3 is Rb dependent and relies on the inhibition of cyclin D1 transcription. *Mol. Cell. Biol.* **20**: 1797–1815.
- Guehenneux, F., Duret, L., Callanan, M. B., Bouhas, R., Hayette, S., Berthet, C., Samarut, C., Rimokh, R., Birot, A. M., Wang, Q., Magaud, J. P., and Rouault, J.-P. (1997). Cloning of the mouse BTG3 gene and definition of a new gene family (the BTG family) involved in the negative control of the cell cycle. *Leukemia* **11**: 370–375.
- Hotz, M. A., Gong, J., Traganos, F., and Darzynkiewicz, Z. (1994). Flow cytometric detection of apoptosis: Comparison of the assays *in situ* DNA degradation and chromatin changes. *Cytometry* **15**: 237–244.
- Iacopetti, P., Barsacchi, G., Tirone, F., Maffei, L., and Cremisi, F. (1994). Developmental expression of PC3 gene is correlated with neuronal cell birthday. *Mech. Dev.* **47**: 127–137.
- Iacopetti, P., Michelini, M., Stuckmann, I., Obach, B., Aaku-Saraste, E., and Huttner, W. B. (1999). Expression of the antiproliferative gene TIS21 at the onset of neurogenesis identifies single neuroep-

- ithelial cells that switch from proliferative to neuron-generating division. *Proc. Natl. Acad. Sci. USA* **96**: 4639–4644.
- Ikematsu, N., Yoshida, Y., Kawamura-Tsuzuku, J., Ohsugi, M., Onda, M., Hirai M., Fujimoto, J., and Yamamoto, T. (1999). Tob2, a novel anti-proliferative Tob/BTG1 family member, associates with a component of the CCR4 transcriptional regulatory complex capable of binding cyclin-dependent kinases. *Oncogene* **18**: 7432–7441.
- Kalejta, R. F., Shenk, T., and Beavis, A. J. (1997). Use of a membrane-localized green fluorescent protein allows simultaneous identification of transfected cells and cell cycle analysis by flow cytometry. *Cytometry* **29**: 286–291.
- Kozak, M. (1984). Compilation and analysis of sequences upstream from the translational start site in eukaryotic mRNAs. *Nucleic Acids Res.* **12**: 857–872.
- Liu, H. Y., Toyn, J. H., Chiang, Y. C., Draper, M. P., Johnston, L. H., and Denis, C. L. (1997). DBF2, a cell cycle-regulated protein kinase, is physically and functionally associated with the CCR4 transcriptional regulatory complex. *EMBO J.* **16**: 5289–5298.
- Matsuda, S., Kawamura-Tsuzuku, J., Ohsugi, M., Yoshida, M., Emi, M., Nakamura, Y., Onda, M., Yoshida, Y., Nishiyama, A., and Yamamoto, T. (1996). Tob, a novel protein that interacts with p185erbB2, is associated with anti-proliferative activity. *Oncogene* **12**: 705–713.
- Montagnoli, A., Guardavaccaro, D., Starace, G., and Tirone, F. (1996). Overexpression of the nerve growth factor-inducible PC3 immediate early gene is associated to inhibition of cell proliferation. *Cell Growth Differ.* **7**: 1327–1336.
- Moulton, D. G. (1974). Dynamics of cell populations in the olfactory epithelium. *Ann. N.Y. Acad. Sci.* **237**: 52–61.
- Pesce, M., Gross, M. K., and Schöler, H. R. (1998). In line with our ancestors: Oct-4 and the mammalian germ. *BioEssays* **20**: 722–732.
- Rouault, J.-P., Falette, N., Guéhenneux, F., Guillot, C., Rimokh, R., Wang, Q., Berthet, C., Moyret-Lalle, C., Savatier, P., Pain, B., Shaw, P., Berger, R., Samarut, J., Magaud, J.-P., Ozturk, M., Samarut, C., and Puisieux, A. (1996). Identification of BTG2, an antiproliferative p53-dependent component of the DNA damage cellular response pathway. *Nat. Genet.* **14**: 482–486.
- Rouault, J.-P., Prevot, D., Berthet, C., Birot, A. M., Billaud, M., Magaud, J.-P., and Corbo, L. (1998). Interaction of BTG1 and p53-regulated BTG2 gene products with mCaf1, the murine homolog of a component of the yeast CCR4 transcriptional regulatory complex. *J. Biol. Chem.* **273**: 22563–22569.
- Rouault, J.-P., Rimokh, R., Tessa, C., Paranhos, G., Ffrench, M., Duret, L., Garoccio, M., Germain, D., Samarut, J., and Magaud, J.-P. (1992). BTG1, a member of a new family of antiproliferative genes. *EMBO J.* **11**: 1663–1670.
- Rouault, J.-P., Samarut, C., Duret, L., Tessa, C., Samarut, J., and Magaud, J. P. (1993). Sequence analysis reveals that the BTG1 anti-proliferative gene is conserved throughout evolution in its coding and 3' non-coding regions. *Gene* **129**: 303–306.
- Schwartz Levey, M., Chikaraishi, D. M., and Kauer, J. S. (1991). Characterization of potential precursor populations in the mouse olfactory epithelium using immunocytochemistry and autoradiography. *J. Neurosci.* **11**: 3556–3564.
- Smart, I. H. M. (1971). Location and orientation of mitotic figures in the developing mouse olfactory epithelium. *J. Anat.* **109**: 243–251.
- Suzuki, Y., and Takeda, M. (1993). Basal cells in the mouse olfactory epithelium during development: Immunohistochemical and electron-microscopic studies. *Brain Res. Dev. Brain Res.* **73**: 107–113.
- Taylor, K. D., and Piko, L. (1990). Quantitative changes in cytoskeletal beta- and gamma-actin mRNAs and apparent absence of sarcomeric actin gene transcripts in early mouse embryos. *Mol. Reprod. Dev.* **26**: 111–121.
- Walter, M. A., Spillet, D. J., Thomas, P., Weissenbach, J., and Goodfellow, P. N. (1994). A method for constructing radiation hybrid maps of whole genomes. *Nat. Genet.* **7**: 22–28.
- Yoshida, Y., Matsuda, S., Ikematsu, N., Kawamura-Tsuzuku, J., Inazawa, J., Umemori, H., and Yamamoto, T. (1998). ANA, a novel member of Tob/BTG1 family, is expressed in the ventricular zone of the developing central nervous system. *Oncogene* **16**: 2687–2693.
- Zaccagnini, G., Maione, B., Lorenzini, R., and Spadafora, C. (1998). Increased production of mouse embryos in in vitro fertilization by preincubating sperm cells with the nuclease inhibitor aurintricarboxylic acid. *Biol. Reprod.* **59**: 1549–1553.